k-t accelerated - conventional								
	SRes1				SRes2			
	linear	*center-out*	*out-center-out*	*random*	*linear*	*center-out*	*out-center-out*	*random*
Peak velocity Vmax (cm/s)								
AA	-3.1 [-37;31]	-30 [-57;-3.8]	-2.7 [-34;28]	-5.8 [-40;29]	-8.8 [-41;24]	-23 [-56;9.3]	-6.3 [-39;26]	-14 [-40;11]
arch	3.7 [-28;36]	-3.6 [-22;15]	7.4 [-27;41]	1.4 [-21;24]	-0.1 [-32;32]	-9.3 [-27;8.2]	1.3 [-18;21]	-2.8 [-29;23]
DA	3.9 [-22;30]	-14 [-43;16]	2.6 [-32;37]	-2.0 [-32;28]	1.5 [-36;39]	-16 [-41;8.9]	-4.0 [-34;26]	-3.2 [-23;16]
Flow peak Qmax (ml/s)								
AA	-10 [-99;79]	-42 [-123;39]	-8.9 [-120;103]	-19 [-81;43]	-14 [-101;72]	-41 [-124;42]	-10 [-83;62]	-23 [-109;63]
DA	-11 [-77;56]	-35 [-99;29]	-11 [-75;54]	-22 [-64;20]	3.2 [-60;66]	-30 [-91;31]	-12 [-73;49]	-21 [-83;40]
Net volume Qnet (ml)								
AA	0.3 [-13;13]	-5.9 [-18;6.3]	0.1 [-16;17]	0.1 [-13;14]	-0.7 [-19;18]	-3.4 [-17;11]	1.1 [-13;15]	0.6 [-16;17]
DA	-1.6 [-7.7;4.4]	-7.0 [-13;-1.2]	-2.3 [-8.4;3.7]	-4.7 [-12;2.8]	0.1 [-6.5;6.6]	-5.7 [-14;2.3]	-2.7 [-13;7.2]	-4.3 [-12;3.4]

Supporting Table S1: Mean biases [limits of agreement] provided by the Bland-Altman analysis for comparison between each k-t accelerated non-respiration controlled dataset and conventional 4D flow MRI in healthy volunteers, for peak velocity (Vmax) in the ascending (AA) and descending (DA) aorta as well the aortic arch, AA and DA flow peak (Qmax) and net volume (Qnet).

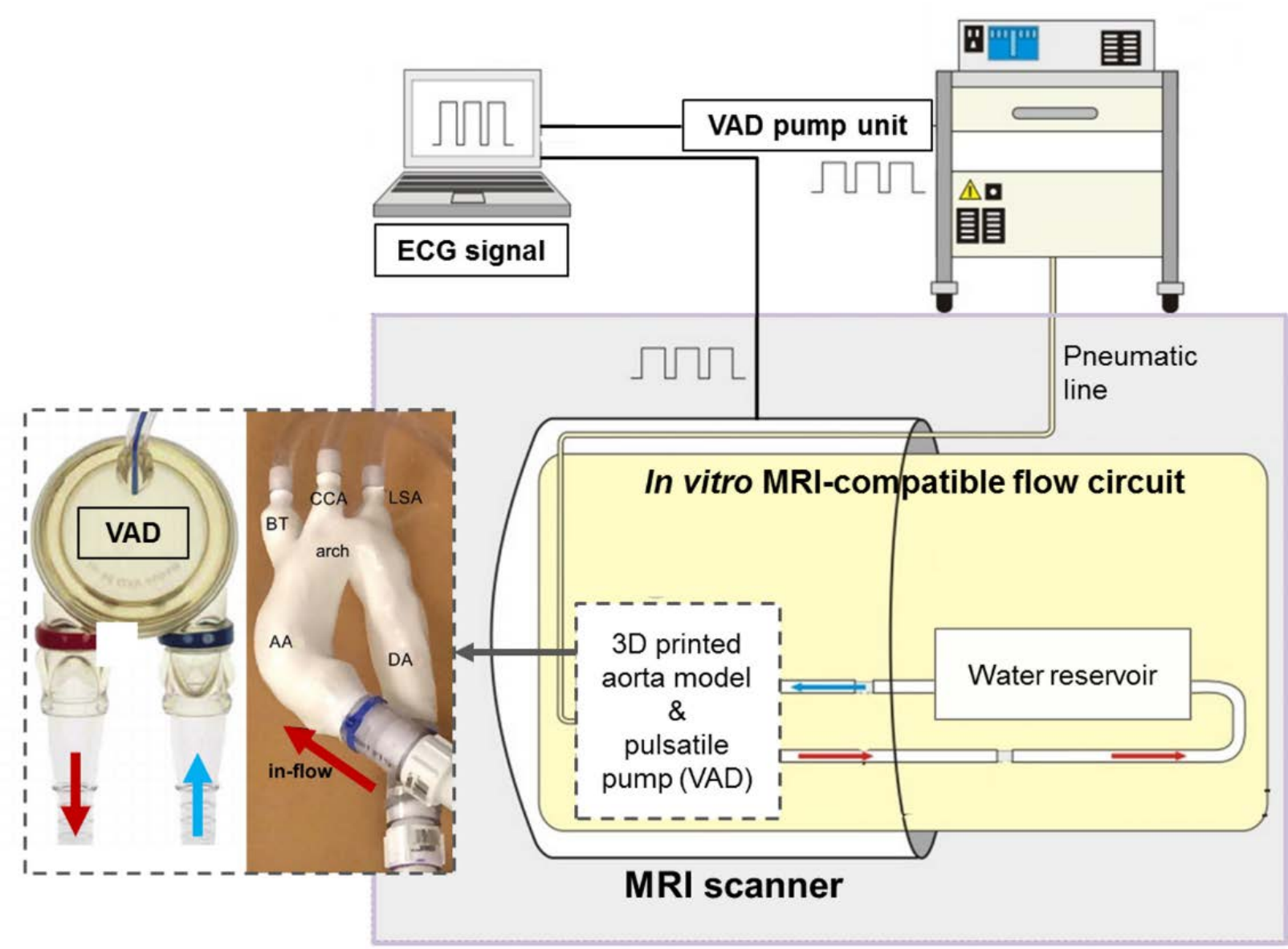

Supporting Figure S1: Experimental setup for *in vitro* 4D flow MRI, including the closed MRI-compatible flow circuit composed of a patient-specific 3D printed aorta model and a pulsatile pump. The ventricular assist device (VAD) pump unit outside of the MRI room controls input to the pump, while synchronized with the ECG gating used for MRI experiment triggering. BT: brachiocephalic trunk; CCA: common carotid artery; LSA: left subclavian artery; AA: ascending aorta; DA: descending aorta.

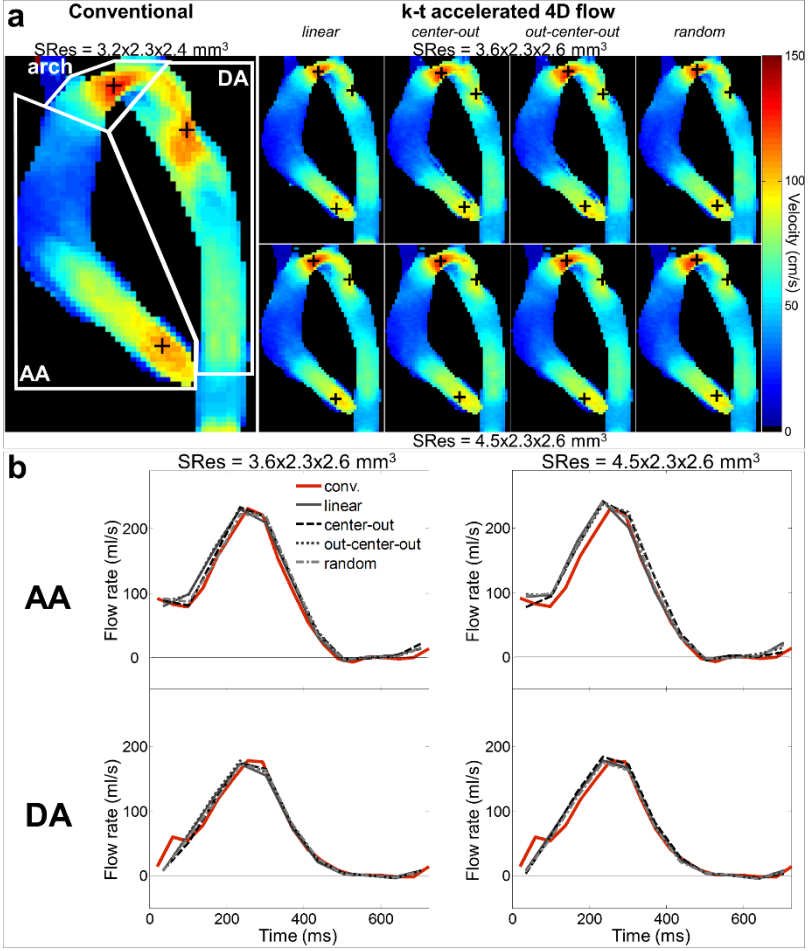

Supporting Figure S2: Comprehensive results of the *in vitro* 4D flow MRI experiments: a) peak systolic velocity maximal intensity projections (MIP) in sagittal orientation as obtained using conventional 4D flow (left) and k-t accelerated 4D flow with all k-space reorderings (linear, 'center-out', 'out-center-out', random) and spatial resolutions of 3.6x2.3x2.6 mm³ (top row) and 4.5x2.3x2.6 mm³ (bottom row). White boxes on the conventional images define ascending (AA) and descending (DA) aorta as well as aortic arch regions. Location of AA, arch and DA peak velocities is indicated by black '+'. b) AA (top row) and DA (bottom row) flow rate waveforms throughout the cardiac cycle, as obtained using conventional 4D flow (in red) and the k-t accelerated 4D flow with all k-space reorderings (see legend) and spatial resolutions (left and right).

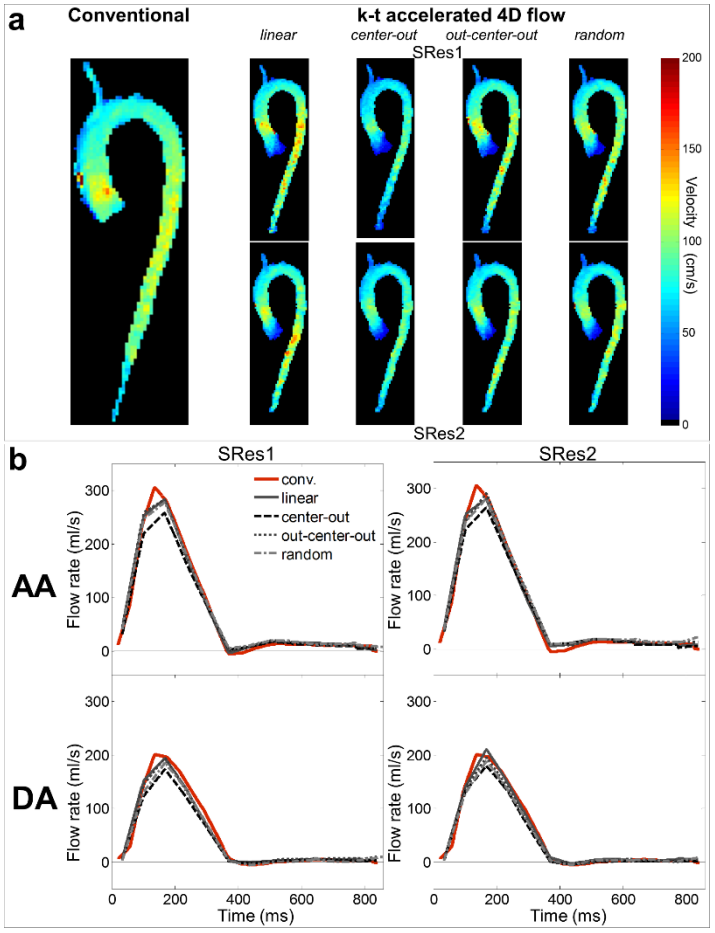

Supporting Figure S3: Comprehensive results of the *in vivo* 4D flow MRI volunteer studies: a) peak systolic velocity maximal intensity projections (MIP) in sagittal orientation as obtained using conventional 4D flow (left) and k-t accelerated 4D flow with all k-space reorderings (linear, 'center-out', 'out-center-out', random) and different spatial resolutions. MIPs were eroded by one pixel to suppress border noise. b) AA (top row) and DA (bottom row) flow rate waveforms throughout the cardiac cycle averaged over the 10 volunteers, as obtained using conventional respiration-controlled 4D flow (in red) and the non-controlled k-t accelerated 4D flow with all k-space reorderings (see legend) and spatial resolutions (lower from left to right).

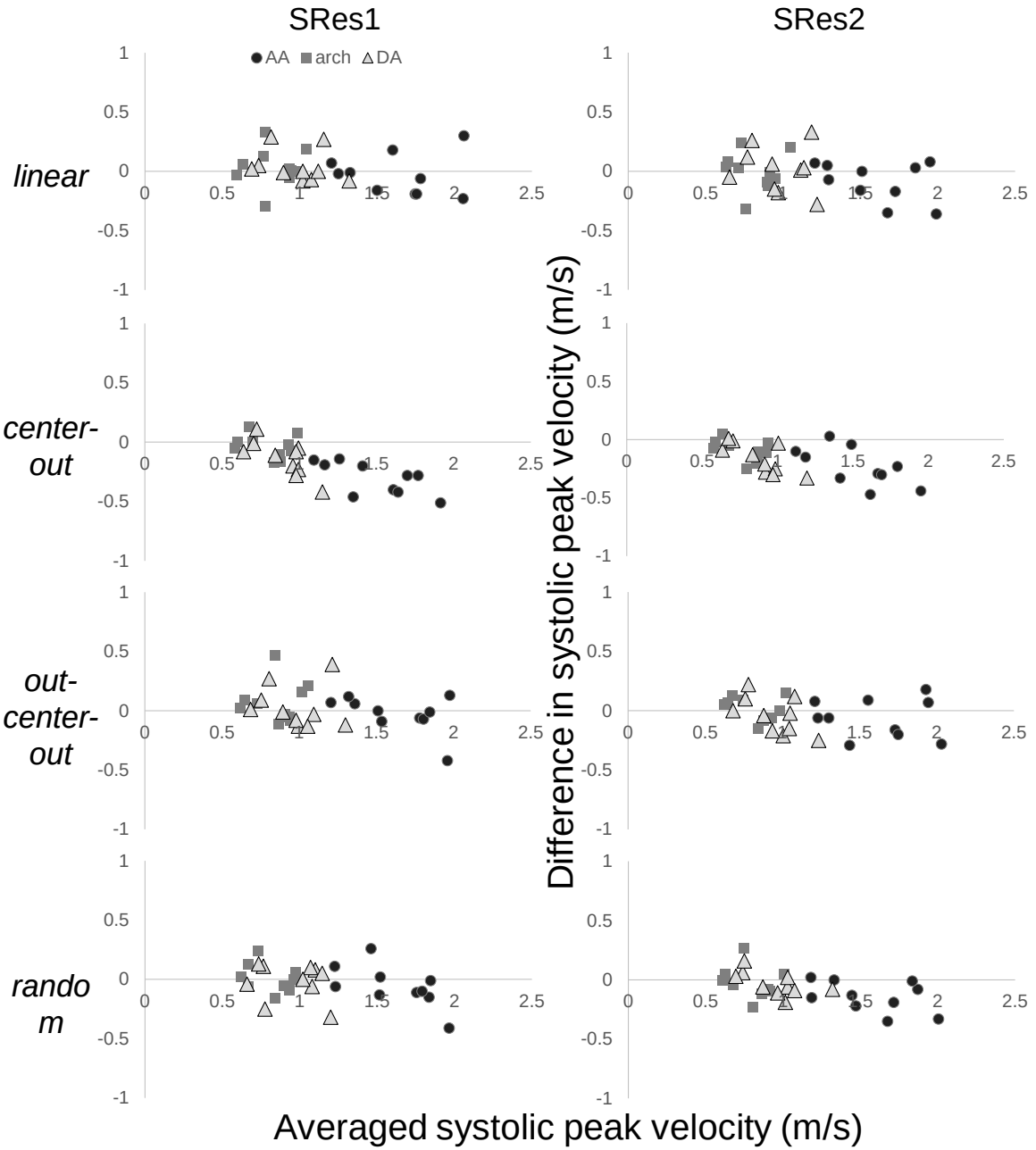

Supporting Figure S4: Bland-Altman diagrams for comparison of peak velocity in the ascending (AA, circles) and descending (DA, triangles) aorta as well in the aortic arch (squares) between k-t accelerated non-respiration controlled datasets and conventional 4D flow MRI in healthy volunteers.

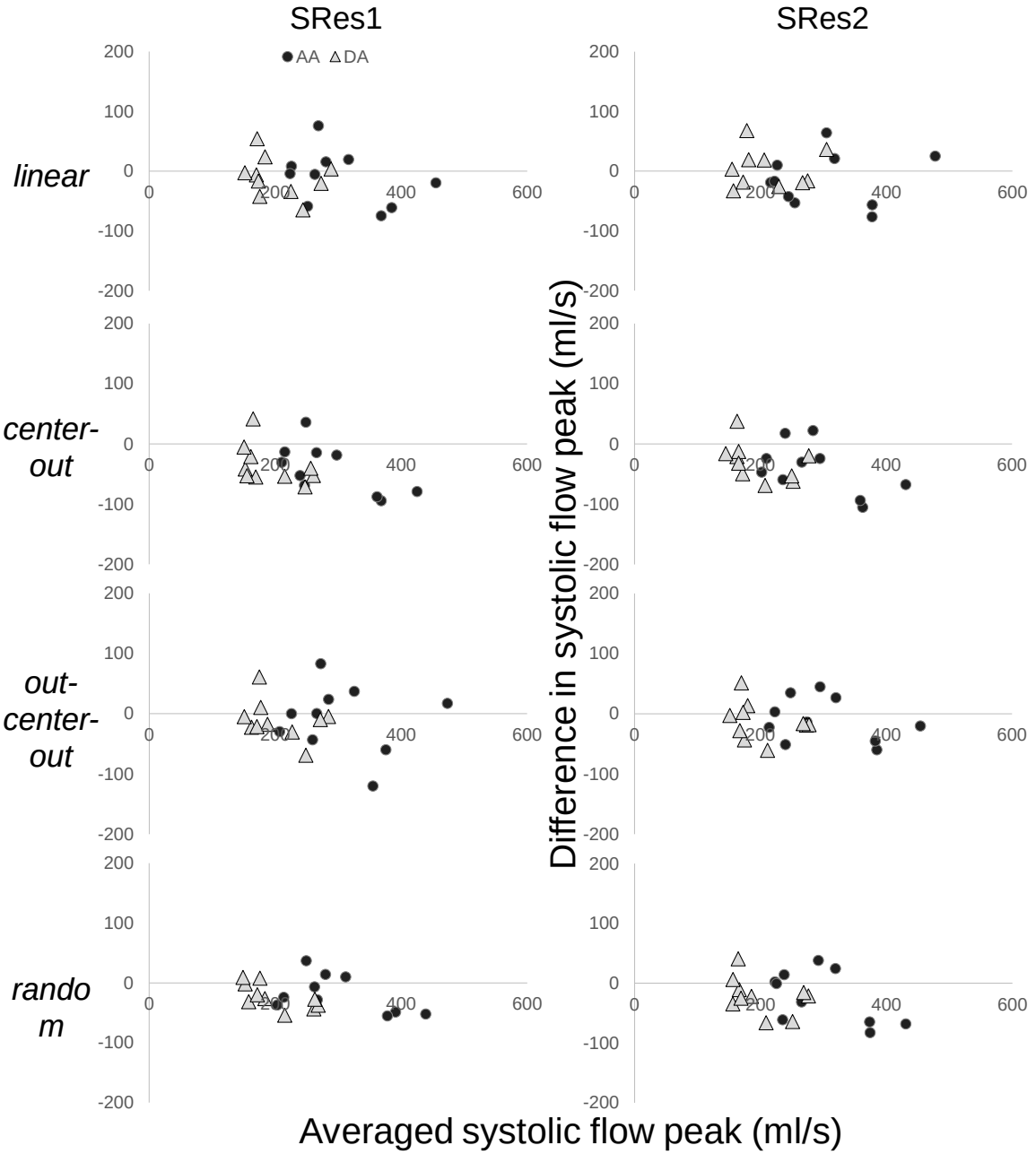

Supporting Figure S5: Bland-Altman diagrams for comparison of peak flow in the ascending (AA, circles) and descending (DA, triangles) aorta between k-t accelerated non-respiration controlled datasets and conventional 4D flow MRI in healthy volunteers.

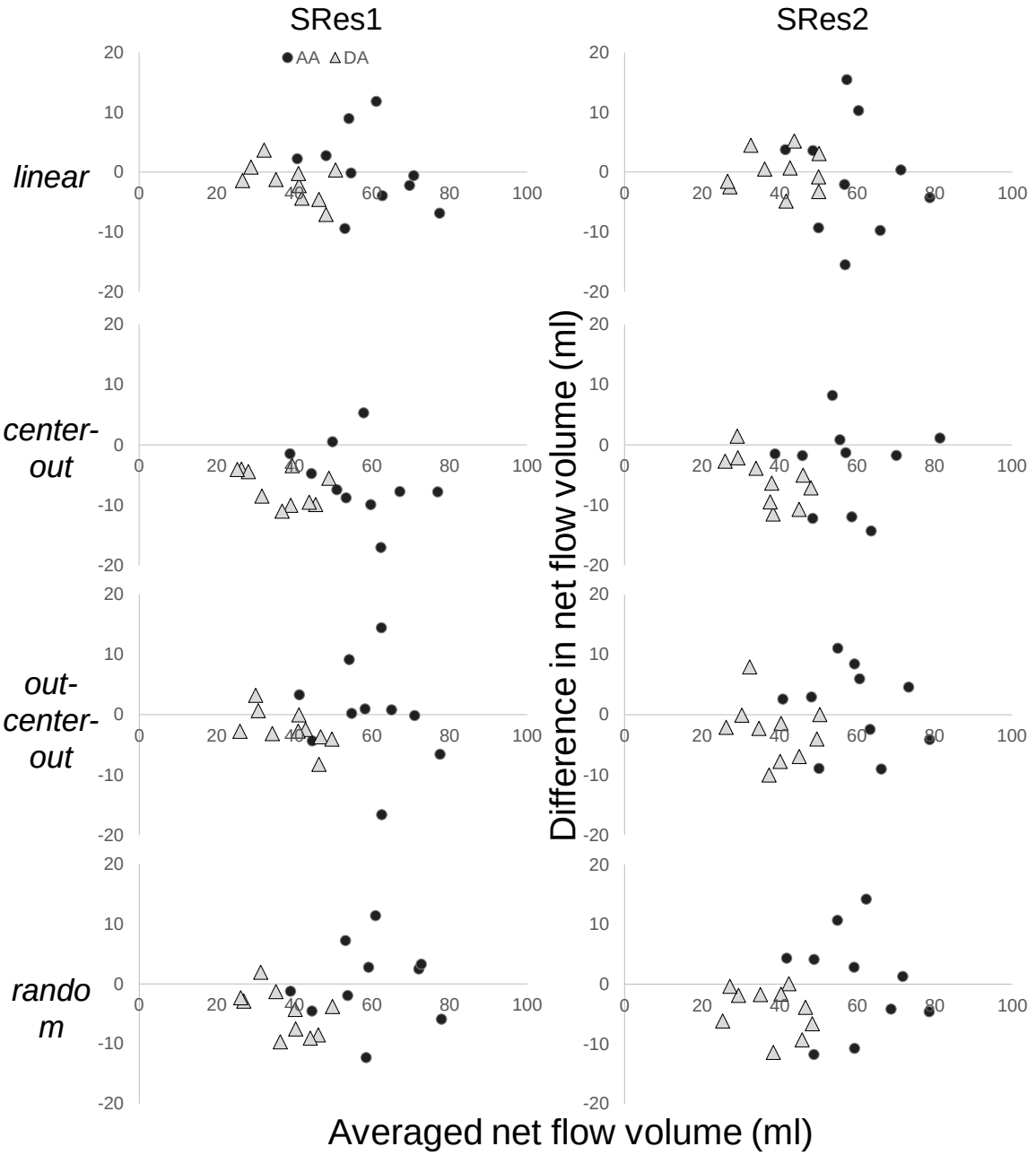

Supporting Figure S6: Bland-Altman diagrams for comparison of net flow volume in the ascending (AA, circles) and descending (DA, triangles) aorta between k-t accelerated non-respiration controlled datasets and conventional 4D flow MRI in healthy volunteers.

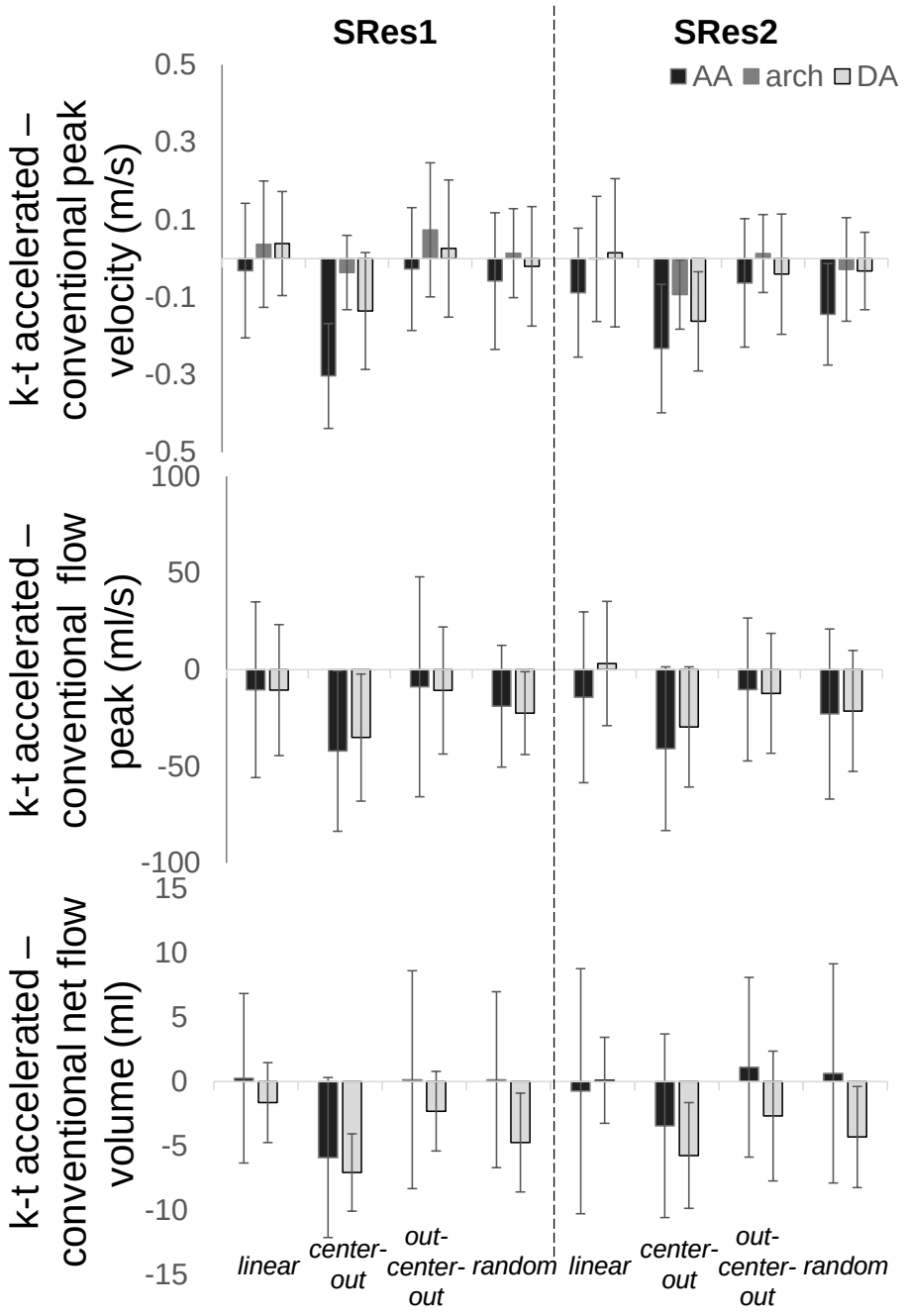

Supporting Figure S7: Comparison between mean biases obtained with k-t accelerated non-respiration controlled datasets vs. conventional 4D flow MRI in healthy volunteers for peak velocity (top), peak flow (middle) and net volume (bottom) in the AA (black), arch (dark grey) and DA (light grey). The bars illustrate difference standard deviations.